Featured in Physics

Order Out of Chaos: Slowly Reversing Mean Flows Emerge from Turbulently Generated Internal Waves

Louis-Alexandre Couston,[1] Daniel Lecoanet,[2] Benjamin Favier,[1] and Michael Le Bars[1]
[1]CNRS, Aix Marseille Univ, Centrale Marseille, IRPHE, Marseille, 13013, France
[2]Princeton Center for Theoretical Science, Princeton, New Jersey 08544, USA

(Received 31 January 2018; published 15 June 2018)

We demonstrate via direct numerical simulations that a periodic, oscillating mean flow spontaneously develops from turbulently generated internal waves. We consider a minimal physical model where the fluid self-organizes in a convective layer adjacent to a stably stratified one. Internal waves are excited by turbulent convective motions, then nonlinearly interact to produce a mean flow reversing on timescales much longer than the waves' period. Our results demonstrate for the first time that the three-scale dynamics due to convection, waves, and mean flow is generic and hence can occur in many astrophysical and geophysical fluids. We discuss efforts to reproduce the mean flow in reduced models, where the turbulence is bypassed. We demonstrate that wave intermittency, resulting from the chaotic nature of convection, plays a key role in the mean-flow dynamics, which thus cannot be captured using only second-order statistics of the turbulent motions.

DOI: 10.1103/PhysRevLett.120.244505

An outstanding question in fluid dynamics is whether large-scale flows can be accurately captured in reduced models that do not resolve fluid motions on small spatio-temporal scales. Reduced models are necessary in many fields of fluid mechanics, since fluid phenomena often occur on a wide range of spatial and temporal scales, preventing exploration via direct numerical simulations (DNSs) of the Navier-Stokes equations. This question is of interest to, for instance, the turbulence community, which has developed closure models in large-eddy simulations and Reynolds-averaged Navier-Stokes simulations [1], the statistical physics and geophysics communities, who aim to describe the self-organization and large-scale behavior of turbulent flows [2–5], and atmospheric and oceanographic scientists, whose goals are to provide long-time predictions of the evolution of our climate using weather-ocean models with coarse resolution [6,7].

A drastic approximation would be to assume that large-scale flows and small-scale motions are dynamically decoupled, but this is rarely the case. A number of important slow large-scale flows are controlled by rapid processes at the small scales. For instance, the 22-yr cycle of solar magnetism is driven by the Sun's convective interior, which evolves on month-long or shorter timescales [8,9]; upwelling of the planetary-scale thermohaline circulation of Earth's oceans hinges on enhanced mixing events that critically depend on small-scale ($\sim$100 m) internal waves [10,11]; Jupiter's zonal jets develop from small-scale turbulence patterns due to convective heat transfers in the weather layer and deep interior [12].

The generation of a large-scale flow by turbulent fluctuations can be studied by spatial averaging the Navier-Stokes equations. Let us consider the case of a large-scale mean flow $\bar{u}$ in the horizontal x direction perpendicular to downward gravity, with overbar denoting the horizontal mean. We write (u', w') the velocity fluctuations in (x, z) directions with $\hat{z}$ the upward vertical axis. In these two dimensions, the horizontal mean of the Navier-Stokes equation in the x direction reads

$$\partial_t \bar{u} - \nu \partial_{zz} \bar{u} = -\partial_z \overline{(w'u')}, \tag{1}$$

with ν the kinematic fluid viscosity. The right-hand side of (1) is minus the divergence of the Reynolds stress and is the momentum source or sink for the mean flow. In isotropic homogeneous turbulence, we do not expect the generation of a mean flow due to the lack of symmetry breaking. However, any inhomogeneity or anisotropy of the fluctuations can initiate a slowly varying mean flow, whose fate depends on its interaction with the fluctuations [4]. The parametrization of the Reynolds stress $\overline{(w'u')}$ for unresolved scales is the key ingredient in all reduced models. Generally, a closure model expresses the Reynolds stresses in terms of the resolved variables [1].

In our case of interest, the small-scale fluctuations are oscillating disturbances of the density field called internal waves. Internal waves are ubiquitous in oceans [13], planetary atmospheres [14–17], stars [18,19], brown dwarves [20], and planetary cores [21]. In the atmosphere, internal waves actively contribute to the generation of mean equatorial winds in Earth's stratosphere, which change direction roughly every 14 months, coined the quasibiennial oscillation (QBO) [22]. Internal waves may also be involved in the generation of reversing zonal flows on

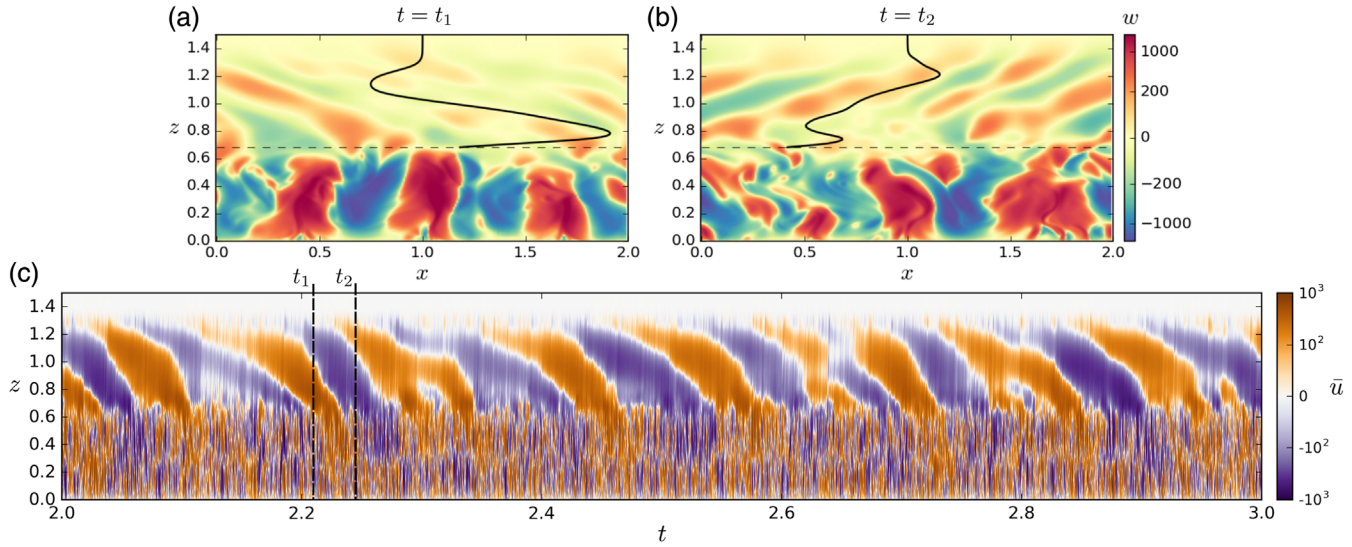

FIG. 1. DNS results. (a), (b) Snapshots of the vertical velocity field w at times $t_1 = 2.21$ and $t_2 = 2.24$, along with the mean flow $\bar{u}$ (solid line) for $z > z_{\mathrm{NB}} = 0.68$ (with $\bar{u} = 0$ corresponding to $x = 1$). Vertical velocity patterns show convective motions in the lower part of the domain ($z \leq z_{\mathrm{NB}}$) and internal-wave motions in the upper part ($z \geq z_{\mathrm{NB}}$). Note that energy propagates upward along wave crests, so crests toward the upper left (right) correspond to retrograde (prograde) waves. (c) The mean flow $\bar{u}(t, z)$. The mean flow in the convective zone corresponds to the average of stochastic plumes emitted from the bottom boundary and hence reverses on a relatively rapid, convective timescale. In the stably stratified layer, $\bar{u}$ results from the nonlinear interaction of internal waves and oscillates on timescales ~ 0.1, much longer than the buoyancy period $\sim \pi 10^{-4}$. Simulation details and videos are available in Supplemental Material [33].

Saturn [23] and Jupiter [24], they are of interest for extrasolar planetary atmospheres [25], and may influence the differential rotation of stars [26] and slow large-scale motions of Earth's magnetic field [27].

Here, we report results of the first DNS of a realistic slowly reversing mean flow emerging from small-scale fluctuations in two dimensions, and we unravel the key physics of the generation mechanism using a hierarchy of low-order models in which the Reynolds stresses are approximated. We use the horizontally periodic self-consistent model of convective-stably stratified dynamics of [28]. The velocity $\boldsymbol{u} = (u, w)$, temperature T, and density anomaly $\rho = -\alpha T$ satisfy the Boussinesq equations

$$\partial_t \boldsymbol{u} + (\boldsymbol{u} \cdot \nabla)\boldsymbol{u} + \nabla p = \mathrm{Pr}\, \nabla^2 \boldsymbol{u} - \mathrm{Pr}\, \mathrm{Ra} \rho \hat{z} - \boldsymbol{u}\tau, \quad (2a)$$

$$\partial_t T + (\boldsymbol{u} \cdot \nabla) T = \nabla^2 T, \quad (2b)$$

$$\nabla \cdot \boldsymbol{u} = 0, \quad (2c)$$

nondimensionalized with κ (thermal diffusivity) and H (characteristic height). The fluid is thermally stratified (T_t and T_b imposed on the top and bottom no-slip boundaries) and exhibits a buoyancy reversal at the inversion temperature T_i with $T_b > T_i > T_t$ (similar to water, whose density maximum is at 4 °C [29]). Thus, the fluid spontaneously organizes into a lower, nearly isothermal convective region and an upper stably stratified region. $\mathrm{Pr} = \nu/\kappa$ and $\mathrm{Ra} = \alpha_s g \Delta T H^3/(\kappa\nu)$ are the Prandtl and global Rayleigh numbers, α_s is the expansion coefficient for $T > T_i$, and $\Delta T > 0$ is the difference between the dimensional bottom and inversion temperatures, such that using $T_i = 0$ as the dimensionless reference temperature, we have $T_b = 1$. The buoyancy reversal is obtained using the nonlinear equation of state for ρ

$$\rho(T) = -\alpha(T) T = \begin{cases} -T, & T \geq T_i = 0, \\ ST, & T \leq T_i = 0, \end{cases} \quad (3)$$

with S the stiffness parameter [28]. We define the neutral buoyancy level z_{NB} to be the height at which adiabatic plumes emitted from the bottom boundary become neutrally buoyant. This roughly corresponds to the height of the convection zone [28,30] or, equivalently, the base of the stable layer [dashed lines in Figs. 1(a) and 1(b)]. The normalized domain lengths are $L_x = 2$ and $L_z = 1.5$ in the x and z directions, which leads to an aspect ratio of the convection at statistical steady state close to 3 for all simulations; $\tau = 10^2\sqrt{2}\{\tanh[(z - L_z + 0.15)/0.05] + 1\}/2$ is a z-dependent linear damping used to prevent wave reflections from the top boundary. We solve equations (2) via DNS using DEDALUS [31] with Chebyshev polynomials (Fourier modes) in the z (x) direction. DNSs are run over several thermal diffusion times in order to allow the system to reach a statistical equilibrium self-consistently and obtain several reversals of the mean flow.

Figure 1 shows the main DNS results of the Letter, obtained for $T_t = -43$, $T_b = 1$, $\mathrm{Pr} = 0.2$, $\mathrm{Ra} = 1.2 \times 10^8$,

and $S = 1/3$, such that the convection-wave coupling is relatively strong and the interface is flexible [28]. With $z_{\mathrm{NB}} = 0.68$, the effective Rayleigh number is $\mathrm{Ra}_{\mathrm{eff}} = z_{\mathrm{NB}}^3 \mathrm{Ra} \approx 4 \times 10^7$. Snapshots of vertical velocity [Figs. 1(a) and 1(b)] reveal large convective updrafts and downflows below z_{NB} and internal waves above. If there was no mean flow in the stably stratified layer, convection would generate pro- and retrograde waves with similar amplitude. However, in Figs. 1(a) and 1(b), the internal waves are mostly propagating in a single direction, an indication that the mean flow (shown by the solid line) is filtering waves going in the opposite direction. The evolution of the mean flow over one thermal timescale is shown in Fig. 1(c). The stable layer has a strong mean flow that reverses every ~0.05 thermal time. Each new mean-flow phase starts near the top of the domain and descends toward the convective layer. The mean flow is driven by wave damping at critical layers and by viscous and thermal dissipation. Critical layers [32] are ubiquitous in our DNS because convection generates a broad spectrum of waves, some of which have low phase velocities. Viscous and thermal dissipation effects are relatively strong in our DNS, so the basic mean-flow mechanism is essentially due to wave dissipation.

Previous studies of wave–mean-flow interactions have focused on momentum deposition by internal waves of a single frequency and wave number [38,39]. In such cases, it can be shown analytically that a slowly reversing mean flow emerges provided that there are both prograde and retrograde waves, as well as an initial disturbance. The prograde (respectively, retrograde) wave provides a $+x$ positive (respectively, negative) acceleration for the mean flow through damping. Then, the competition of the two forces (whose intensity depends on the direction of the mean flow through the Doppler shift) leads to the observed long-time oscillation of $\bar{u}$ [22].

Our results demonstrate for the first time that an oscillating mean flow can emerge from internal waves generated by turbulent motions with no control over the waves (i.e., no parametrization). Importantly, the fundamental mechanism that applies for monochromatic waves also applies for a broadband spectrum of internal waves: damping and momentum deposition is stronger for waves going in the same direction as the mean flow. This is shown in Fig. 1(a), where a strong mean flow in the positive direction strongly dissipates prograde waves, such that only retrograde waves can be visible above. The same is true in Fig. 1(b), but for the case of a negative mean flow. With a broadband spectrum of waves, whose amplitudes can vary over time due to the chaotic dynamics of convection, momentum deposition cannot be simply traced back to a handful of self-interaction terms in the Reynolds stress that would be coherent over long times. Driving of a mean flow in this context may be unexpected, but is in fact generic at sufficiently low Pr: as Fig. 2 shows, the mean flow becomes stronger and more regular as Pr decreases.

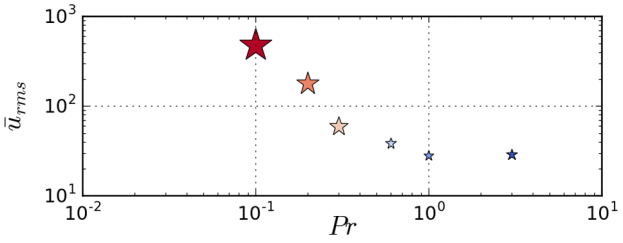

FIG. 2. Mean-flow rms $\bar{u}_{\mathrm{rms}}$ as a function of Pr. The mean flow becomes stronger as Pr decreases and is also more regular: the symbols' area is inversely proportional to the frequency bandwidth of $\bar{u}$, defined as the difference $\Delta f = f_{0.9} - f_{0.1}$ of the two frequencies $f_{0.1}$ and $f_{0.9}$ below and above which lies 10% of the mean-flow energy.

This can be understood from the fact that, while the forcing through wave damping is only weakly affected by decreasing Pr (because waves are damped through both viscous and thermal dissipation effects), the mean flow experiences much less dissipation (it is only damped through viscosity effects), hence becoming stronger. As a result, wave-driven flows should emerge relatively easily in low-Prandtl-number fluids, such as planetary cores made of liquid metal and stellar interiors [40,41], potentially affecting planetary and stellar dynamos [42] and magnetic reversals [43,44].

We now compare results of the full DNS model for the parameters of Fig. 1 (denoted by $\mathbf{M}_1$) with results obtained from two reduced models ($\mathbf{M}_2$ and $\mathbf{M}_3$), described in Fig. 3(a). The goal of the reduced models is to reproduce the evolution of the mean flow without resolving the convection. $\mathbf{M}_{2,3}$ only solve the dynamics of the stable layer and are forced by prescribing values for the flow variables at its base (z_{NB}). If we force with exact time-varying values of (u', w') and T' from the full DNS, the evolution of $\bar{u}$ is exactly reproduced in $\mathbf{M}_2$ (not shown). Observations of real systems do not generally provide information about all variables at sufficient temporal and spatial resolution over long time periods, so we only use a subset of the full DNS data to force the reduced models. Specifically, here we expand the fluctuations u', w', T' in $\mathbf{M}_{2,3}$ in series of linear internal-wave modes, and we set their amplitudes such that the kinetic energy of each wave mode (defined by each wave's frequency ω and wave number k) matches the kinetic energy spectrum $\mathcal{K}(\omega, k)$ obtained in the full DNS at z_{NB}. Note that we could have set the shape of the internal-wave spectrum using theoretical predictions for the wave generation by turbulent convection [45,46], but that would preclude a comparison to $\mathbf{M}_1$, whose wave spectrum differs from, e.g., [45,46].

The reduced models only differ in how wave propagation away from the bottom boundary is solved. In $\mathbf{M}_2$, wave propagation is solved exactly by DNS of the Boussinesq equations, while in $\mathbf{M}_3$, a closed-form solution for the Reynolds stress is derived such that we only solve the 1D mean flow equation (1). The analytical solution for the fluctuations (u', w') in $\mathbf{M}_3$ is obtained through WKB

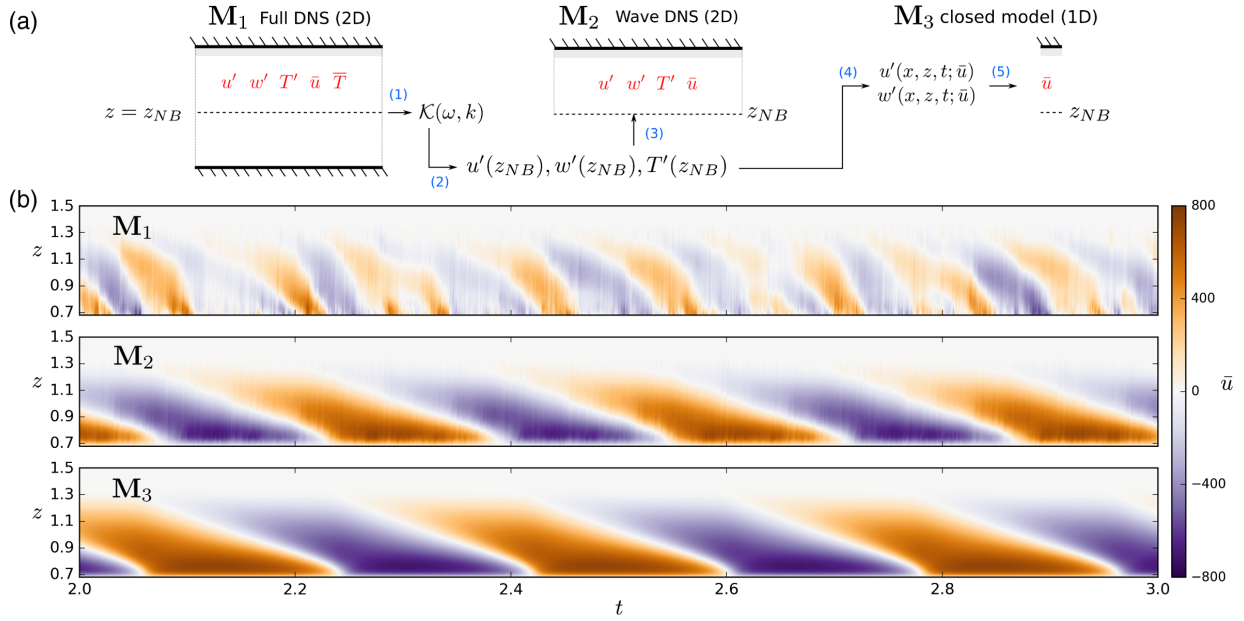

FIG. 3. (a) Schematics of the DNS model $\mathbf{M}_1$ and the two reduced models $\mathbf{M}_2$ and $\mathbf{M}_3$. (1) We calculate the kinetic energy spectrum $\mathcal{K}$ of the fluctuations at height z_{NB} obtained in $\mathbf{M}_1$. (2) The forcing (u', w', T') is derived from $\mathcal{K}$, assuming that the fluctuations correspond to linear propagating internal waves. Propagation of the waves is solved (3) via DNS of the Boussinesq equations in $\mathbf{M}_2$, but is derived analytically (4) in $\mathbf{M}_3$ under WKB approximation. Thus, in $\mathbf{M}_3$ (5), we only need to solve for the mean-flow equation. As in full DNS, we use a damping layer for $1.35 < z < 1.5$, and boundary conditions for the mean flow are no slip. (b) $\bar{u}$ over one thermal time obtained for each model shown in (a). Physical parameters are as in Fig. 1. Note that the colormap has been changed in Fig. 3(b) compared to Fig. 1(c) to highlight differences between $\mathbf{M}_1$ and $\mathbf{M}_{2,3}$.

approximation, neglecting nonlinear wave-wave terms, mean-flow acceleration, and cross-interaction terms in the Reynolds stress (cf. details in the Supplemental Material [33]). We note that, while $\mathbf{M}_2$ is computationally cheaper than $\mathbf{M}_1$ (resolution is 8 times smaller and time steps are $\sim$3 times larger), it remains significantly more demanding than $\mathbf{M}_3$, which is the only practical model for predicting the long-term dynamics of real systems (e.g., capturing the QBO in General Circulation Models). The goal of $\mathbf{M}_2$ is to check approximations made in $\mathbf{M}_3$.

Figure 3(b) shows the temporal variations of the mean flow $\bar{u}$ obtained in full DNS $\mathbf{M}_1$ and in the two reduced models $\mathbf{M}_2$ and $\mathbf{M}_3$. A large-scale oscillation is obtained in all three models, but the mean flow is stronger and the period is longer in the reduced models than in full DNS. Let us consider the characteristic amplitude of the mean flow by its rms ($\bar{u}_{\mathrm{rms}}$) and the characteristic period by taking the inverse of the peak frequency of its Fourier transform ($T_{\bar{u}}$), which we average vertically between $z = 0.8$ and 1.1. We have $\bar{u}_{\mathrm{rms}} = 179$ ($\mathbf{M}_1$), 370 ($\mathbf{M}_2$), and 415 ($\mathbf{M}_3$), $T_{\bar{u}} = 0.125$ ($\mathbf{M}_1$), $\approx$0.33 ($\mathbf{M}_2$), and $\approx$0.33 ($\mathbf{M}_3$). Clearly, even when the wave propagation is solved exactly by DNS ($\mathbf{M}_2$), the mean-flow dynamics is not reproduced quantitatively. In addition, some of the temporal variability of the mean flow obtained in full DNS is lacking in both reduced models.

The large discrepancy between the reduced models and DNS comes from the assumption that fluctuations on the lower boundary $z = z_{\mathrm{NB}}$ of $\mathbf{M}_{2,3}$ can be reconstructed from the time-averaged spectrum $\mathcal{K}$ using the linear wave relations for upward propagating plane waves. However, $\mathcal{K}$ can include contributions from overshooting plumes and some of the waves may be nonlinear. In our $\mathbf{M}_1$ ($\mathbf{M}_2$) simulations, the nonlinear terms have a typical magnitude of approximately 50% (10%) of the linear terms just above z_{NB}, suggesting overshooting convection in $\mathbf{M}_1$ may be non-negligible at the interface. However, in the bulk of the stable region, this decreases to about 10% (5%), so the waves are in a weakly nonlinear regime (cf. details in the Supplemental Material [33]). Because the waves are weakly nonlinear, the energy transfer among waves does not affect the mean flow, explaining the agreement between $\mathbf{M}_2$ and $\mathbf{M}_3$. Because forcing using the spectrum higher than z_{NB} could in principle attenuate contributions from nonlinear convective motions, we have run additional simulations with different forcing heights (cf. Fig. S2 of the Supplemental Material [33]): quantitative changes for the mean flow are obtained, but never lead to agreement with full DNS results. Importantly, the reconstruction of wave fluctuations from an energy spectrum neglects high-order statistics (higher than 2), so statistics in the reduced models are Gaussian. However, intermittent events exist near the interface because the convection does not have a top-down symmetry and exhibits non-Gaussian statistics. In fact, the kurtosis of the fluctuations remains large, even in the wave field far from the interface z_{NB} (see Fig. S3 of

the Supplemental Material [33]), suggesting that intermittency is a key component of wave generation. Intermittent intense wave events found in our DNS but neglected in the reduced models are typical of real systems. In the Atmosphere, for instance, atmospheric waves sometimes propagate in the form of localized wave packets [47], such that wave intermittency can be non-negligible and has to be incorporated in reduced mean-flow models using stochastic processes [48].

In conclusion, the spontaneous generation and oscillation of a mean flow in our minimal, physical model is obtained for a wide range of parameters. In particular, we find that the mean flow becomes stronger as Pr decreases (Fig. 2), which highlights the necessity to account for the real value of Pr in stellar and planetary dynamical models. Evaluating the impact of wave-driven flows in natural systems is challenging. Indeed, we have shown here that reduced models do not yet predict the correct physics: tackling simultaneously the three-scale dynamics due to turbulence, waves, and mean flow seems necessary. A major source of errors in reduced models comes from the approximations made in the types of waves excited by convection, even if the stably stratified layer is forced with waves with the same kinetic energy spectrum as in full DNS. Our analysis suggests that implementing wave intermittency (through a boundary forcing scheme that would match the high-order moments of the DNS statistics) and disentangling nonwave contributions from the source spectrum are the next step forward and will be essential to improve the long-time predictive capabilities of low-order models.

The authors acknowledge funding by the European Research Council under the European Union's Horizon 2020 research and innovation program through Grant No. 681835-FLUDYCO-ERC-2015-CoG. D. L. is supported by a PCTS fellowship and a Lyman Spitzer Jr fellowship. LAC thanks Bruno Ribstein for useful discussions and references on parametrizations in General Circulation Models. Computations were conducted with support by the HPC resources of GENCI-IDRIS (Grant No. A0020407543 and A0040407543) and by the NASA High End Computing (HEC) Program through the NASA Advanced Supercomputing (NAS) Division at Ames Research Center on Pleiades with allocations GID s1647 and s1439.

[1] P. A. Durbin, Some recent developments in turbulence closure modeling, Annu. Rev. Fluid Mech. **50**, 77 (2018).
[2] F. Bouchet and A. Venaille, Statistical mechanics of two-dimensional and geophysical flows, Phys. Rep. **515**, 227 (2012).
[3] J. B. Marston, G. P. Chini, and S. M. Tobias, Generalized Quasilinear Approximation: Application to Zonal Jets, Phys. Rev. Lett. **116**, 214501 (2016).
[4] S. Fauve, J. Herault, G. Michel, and F. Pétrélis, Instabilities on a turbulent background, J. Stat. Mech. (2017) 064001.
[5] A. Pouquet and R. Marino, Geophysical Turbulence and the Duality of the Energy Flow Across Scales, Phys. Rev. Lett. **111**, 234501 (2013).
[6] P. Bauer, A. Thorpe, and G. Brunet, The quiet revolution of numerical weather prediction, Nature (London) **525**, 47 (2015).
[7] M. C. Buijsman, J. K. Ansong, B. K. Arbic, J. G. Richman, J. F. Shriver, P. G. Timko, A. J. Wallcraft, C. B. Whalen, and Z. Zhao, Impact of parameterized internal wave drag on the semidiurnal energy balance in a global ocean circulation model, J. Phys. Oceanogr. **46**, 1399 (2016).
[8] D. H. Hathaway, The solar cycle, Living Rev. Solar Phys. **7**, 1 (2010).
[9] P. D. Mininni, D. O. Gómez, and G. B. Mindlin, Biorthogonal Decomposition Techniques Unveil the Nature of the Irregularities Observed in the Solar Cycle, Phys. Rev. Lett. **89**, 061101 (2002).
[10] K. L. Polzin, J. M. Toole, J. R. Ledwell, and R. W. Schmitt, Spatial variability of turbulent mixing in the abyssal ocean, Science **276**, 93 (1997).
[11] M. Nikurashin and R. Ferrari, Overturning circulation driven by breaking internal waves in the deep ocean, Geophys. Res. Lett. **40**, 3133 (2013).
[12] S. Cabanes, J. Aurnou, B. Favier, and M. Le Bars, A laboratory model for deep-seated jets on the gas giants, Nat. Phys. **13**, 387 (2017).
[13] C. Garrett and W. Munk, Internal waves in the ocean, Annu. Rev. Fluid Mech. **11**, 339 (1979).
[14] D. C. Fritts and M. J. Alexander, Gravity wave dynamics and effects in the middle atmosphere, Rev. Geophys. **41**, 1003 (2003).
[15] S. D. Miller, W. C. Straka III, J. Yue, S. M. Smith, M. J. Alexander, L. Hoffmann, M. Setvák, and P. T. Partain, Upper atmospheric gravity wave details revealed in nightglow satellite imagery, Proc. Natl. Acad. Sci. U.S.A. **112**, E6728 (2015).
[16] S. Tellmann, M. Pätzold, B. Häusler, D. P. Hinson, and G. L. Tyler, The structure of Mars lower atmosphere from Mars Express Radio Science (MaRS) occultation measurements, J. Geophys. Res. **118**, 306 (2013).
[17] A. Piccialli, D. V. Titov, A. Sanchez-Lavega, J. Peralta, O. Shalygina, W. J. Markiewicz, and H. Svedhem, High latitude gravity waves at the Venus cloud tops as observed by the Venus monitoring camera on board Venus Express, Icarus **227**, 94 (2014).
[18] C. Charbonnel and S. Talon, Mixing a stellar cocktail, Science **318**, 922 (2007).
[19] T. Straus, B. Fleck, S. M. Jefferies, G. Cauzzi, S. W. McIntosh, K. Reardon, G. Severino, and M. Steffen, The energy flux of internal gravity waves in the lower solar atmosphere, Astrophys. J. Lett. **681**, L125 (2008).
[20] A. P. Showman and Y. Kaspi, Atmospheric dynamics of brown dwarfs and directly imaged giant planets, Astrophys. J. **776**, 85 (2013).
[21] B. Buffett, Geomagnetic fluctuations reveal stable stratification at the top of the Earth's core, Nature (London) **507**, 484 (2014).

[22] M. P. Baldwin, L. J. Gray, T. J. Dunkerton, K. Hamilton, P. H. Haynes, W. J. Randel, J. R. Holton, M. J. Alexander, I. Hirota, T. Horinouchi, D. B. A. Jones, J. S. Kinnersley, C. Marquardt, K. Sato, and M. Takahashi, The quasi-biennial oscillation, Rev. Geophys. **39**, 179 (2001).

[23] G. S. Orton *et al.*, Semi-annual oscillations in Saturn's low-latitude stratospheric temperatures, Nature (London) **453**, 196 (2008).

[24] C. B. Leovy, A. J. Friedson, and G. S. Orton, The quasiquadrennial oscillation of Jupiter's equatorial stratosphere, Nature (London) **354**, 380 (1991).

[25] C. Watkins and J. Y-K. Cho, Gravity waves on hot extrasolar planets. I. Propagation and interaction with the background, Astrophys. J. **714**, 904 (2010).

[26] T. M. Rogers, D. N. C. Lin, and H. H. B. Lau, Internal gravity waves modulate the apparent misalignment of exoplanets around hot stars, Astrophys. J. **758**, L6 (2012).

[27] P. W. Livermore, R. Hollerbach, and C. C. Finlay, An accelerating high-latitude jet in Earth's core, Nat. Geosci. **10**, 62 (2017).

[28] L.-A. Couston, D. Lecoanet, B. Favier, and M. Le Bars, Dynamics of mixed convective–stably-stratified fluids, Phys. Rev. Fluids **2**, 094804 (2017).

[29] M. Le Bars, D. Lecoanet, S. Perrard, A. Ribeiro, L. Rodet, J. M. Aurnou, and P. Le Gal, Experimental study of internal wave generation by convection in water, Fluid Dyn. Res. **47**, 045502 (2015).

[30] D. Lecoanet, J. Schwab, E. Quataert, L. Bildsten, F. X. Timmes, K. J. Burns, G. M. Vasil, J. S. Oishi, and B. P. Brown, Turbulent chemical diffusion in convectively bounded carbon flames, Astrophys. J. **832**, 71 (2016).

[31] K. J. Burns, G. M. Vasil, J. S. Oishi, D. Lecoanet, B. P. Brown, and E. Quataert, Dedalus: A flexible pseudo-spectral framework for solving partial differential equations (unpublished).

[32] J. R. Booker and F. P. Bretherton, The critical layer for internal gravity waves in a shear flow, J. Fluid Mech. **27**, 513 (1967).

[33] See Supplemental Material at http://link.aps.org/supplemental/10.1103/PhysRevLett.120.244505 for details on the models, the effect of the Prandtl number, statistics, and nonlinearities, which includes Refs. [28,31,34–37].

[34] R. S. Lindzen and J. R. Holton, A theory of the quasi-biennial oscillation, J. Atmos. Sci. **25**, 1095 (1968).

[35] R. A. Plumb, The interaction of two internal waves with the mean flow: implications for the theory of the quasi-biennial oscillation, J. Atmos. Sci. **34**, 1847 (1977).

[36] G. K. Vallis, *Atmospheric and Oceanic Fluid Dynamics: Fundamentals and Large-Scale Circulation* 2nd ed. (Cambridge University Press, Cambridge, England, 2017).

[37] U. M. Ascher, S. J. Ruuth, and R. J. Spiteri, Implicit-explicit Runge-Kutta methods for time-dependent partial differential equations, Applied Numerical Mathematics **25**, 151 (1997).

[38] R. A. Plumb and A. D. McEwan, The instability of a forced standing wave in a viscous stratified fluid: a laboratory analogue of the quasi-biennial oscillation, J. Atmos. Sci. **35**, 1827 (1978).

[39] B. Semin, G. Facchini, F. Pétrélis, and S. Fauve, Generation of a mean flow by an internal wave, Phys. Fluids **28**, 096601 (2016).

[40] E. J. Kaplan, N. Schaeffer, J. Vidal, and P. Cardin, Subcritical Thermal Convection of Liquid Metals in a Rapidly Rotating Sphere, Phys. Rev. Lett. **119**, 094501 (2017).

[41] E. M. King and J. M. Aurnou, Turbulent convection in liquid metal with and without rotation, Proc. Natl. Acad. Sci. U.S.A. **110**, 6688 (2013).

[42] L. M. Malyshkin and S. Boldyrev, Magnetic Dynamo Action at Low Magnetic Prandtl Numbers, Phys. Rev. Lett. **105**, 215002 (2010).

[43] V. Carbone, L. Sorriso-Valvo, A. Vecchio, F. Lepreti, P. Veltri, P. Harabaglia, and I. Guerra, Clustering of Polarity Reversals of the Geomagnetic Field, Phys. Rev. Lett. **96**, 128501 (2006).

[44] R. Benzi and J. F. Pinton, Magnetic Reversals in a Simple Model of Magnetohydrodynamics, Phys. Rev. Lett. **105**, 024501 (2010).

[45] P. Goldreich and P. Kumar, Wave generation by turbulent convection, Astrophys. J. **363**, 694 (1990).

[46] D. Lecoanet and E. Quataert, Internal gravity wave excitation by turbulent convection, Mon. Not. R. Astron. Soc. **430**, 2363 (2013).

[47] A. Hertzog, M. J. Alexander, and R. Plougonven, On the intermittency of gravity wave momentum flux in the stratosphere, J. Atmos. Sci. **69**, 3433 (2012).

[48] F. Lott and L. Guez, A stochastic parameterization of the gravity waves due to convection and its impact on the equatorial stratosphere, J. Geophys. Res. **118**, 8897 (2013).